International Conference on Space Optics—ICSO 2018

Chania, Greece

9–12 October 2018

Metal mirror based VIS freeform telescope with smart integration approach

Matthias Beier

Stefan Risse

Wolfgang Holota

Christoph Straif

et al.

METAL MIRROR BASED VIS FREEFORM TELESCOPE WITH SMART INTEGRATION APPROACH

Matthias Beier[1*], Stefan Risse[1], Wolfgang Holota[2], Christoph Straif[3], Sebastian Fischer[3]

[1] Fraunhofer Institut für Angewandte Optik und Feinwerktechnik, Albert-Einstein-Str. 7, 07745 Jena, Germany
[2] Holota Optics, Breitensteinstraße 6, 83727 Neuhaus / Schliersee, Germany
[3] Deutsches Zentrum für Luft- und Raumfahrt, Linder Höhe, 51147 Köln, Germany

ABSTRACT

Modern optical telescopes for Earth observation and remote sensing operations often rely on off-axis mirror designs with aspheric or free-shaped surfaces in order to generate an unobscured image while at the same time covering a large field of view and maintaining an excellent system quality. Continuous improvements in manufacturing and test methods allow for the fabrication of freeform surfaces with low tolerances on figure and roughness. We describe the development, fabrication, and testing of an anamorphic imaging four mirror freeform telescope that operates diffraction limited at visible wavelengths. Based on fabrication and test techniques developed, figure errors of each optical freeform surface were reduced to < 12 nm rms. Roughness values < 0,5 nm rms have been realized based on the applied polishing processes. The optomechanical design of the telescope aims at a minimum of integration effort, reducing the relevant degrees of freedom during mirror alignment from 24 to 3 only and thus allowing for a total system integration within one single day. The telescope concept ensures a reproducible integration and therefore allows for a multi-stage integration after different manufacturing steps in order to correlate surface errors of different spatial frequency with observed wave aberrations on system level. The final experimentally obtained wave aberration is in excellent agreement to the optical design.

I. INTRODUCTION

Small and medium-sized reflective optical devices to be used within both Earth and space-based scientific instrumentation require for precise, cost-effective, and flexible approaches for manufacturing and integration. Ongoing tendencies towards compact, lightweight, and high-resolution optical instruments have a strong impact on the overall concept and optomechanical layout of imaging systems. Furthermore, rise of freeform optical elements led to considerable developments in the field of component fabrication and testing during the last years, which makes them attractive as a meaningful part for future missions [1]. Because of the lack of rotational symmetry, registration and integration of the single freeform surfaces to the common mechanical bench are crucial to avoid time-consuming iterative alignment steps. Metals and particularly aluminum based optical elements, by their nature, are flexibly machinable by diamond turning technologies and integrated at precisely turned or milled interfaces [2]. Tolerances and surface qualities achieved within diamond machining makes these optics directly applicable for near to long IR wavelengths, as used within numerous mid-sized scientific space instruments such as the Mid-Infrared Instrument MIRI [3] and the Fine Guidance Sensor FGS [4] on the James Webb Space Telescope JWST, the Mercury radiometer and thermal infrared spectrometer MERTIS [5], as well as cryogenic optics for Earth-based astronomy, e.g. the high-resolution IR Echelle spectrometer CRIRES at the Very Large Telescope VLT [6].

Metal mirrors applied within VIS operating instruments oftentimes refer to multi- and hyperspectral surveillance and remote sensing operations [7, 8]. The naturally tighter tolerances regarding single element's figure and roughness are fulfilled by plating the aluminum mirrors with a thick layer of amorphous nickel-phosphorous, which can be diamond turned, figure corrected, and polished to excellent surface qualities [9]. A transfer of manufacturing, testing, and integration concepts developed for IR aluminum optics [10, 11] gives possibilities to simplify the production of freeform VIS telescopes and enables a time and cost adapted system development. Appearing issues, like a gaining impact of regular mid-spatial-frequency errors and environmental process control during manufacturing, have to be assessed and faced appropriately by using suitable machining approaches and compensation strategies.

The telescope described within the following article combines freeform manufacturing and testing technologies with a snap-together assembly as known from IR optical instruments [12]. The whole optical and mechanical layout as well as the integration strategy is based on a modular approach that basically brakes down the structure to three final components, namely two optical platforms carrying two freeform mirrors each and a telescope housing. Manufacturing approaches for mirror components and the telescope housing have already been described within previous publications [13, 14]. Within this article, we concentrate on the optical system test and the correlations between residual surface errors on component level and corresponding wavefront errors on system level. In addition, further strategies using a "perfectly bad" mirror surface will be demonstrated [15, 16].

II. OPTOMECHANICAL DESIGN

The optical telescope design uses four off-axis biconic mirrors to transform a rectangular 50 mm x 200 mm entrance pupil into a 70 mm x 70 mm exit pupil (see Fig. 1). The exit pupils for the X and Y directions are located in the same plane, providing full symmetry for possible following instruments. Imaging of the large Y dimension ensures a high resolution, whereas imaging of the smaller X dimension guarantees for a larger field of view. Based on the four anamorphic aspheric mirrors, the design was developed for a wavelength range between 200 nm and 20 µm and achieves diffraction limited performance over most of the central field of view at the testing wavelength λ = 632,8 nm (Fig. 2).
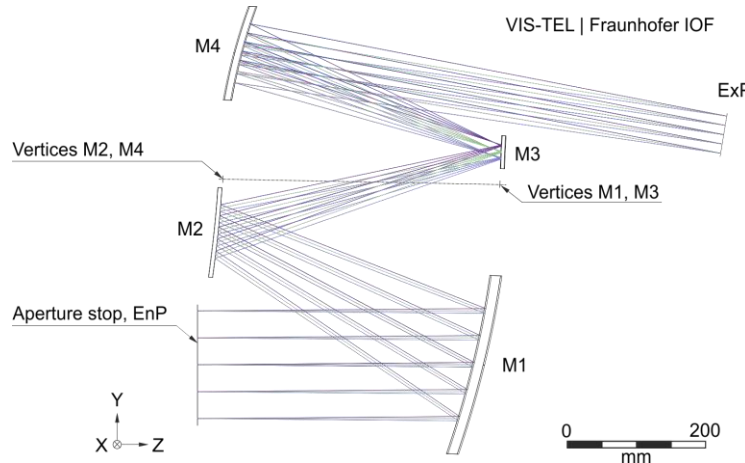

Fig. 1: Optical telescope design. All four mirrors are anamorphic off-axis aspheres. The vertices of each surface lie on a common reference axis.
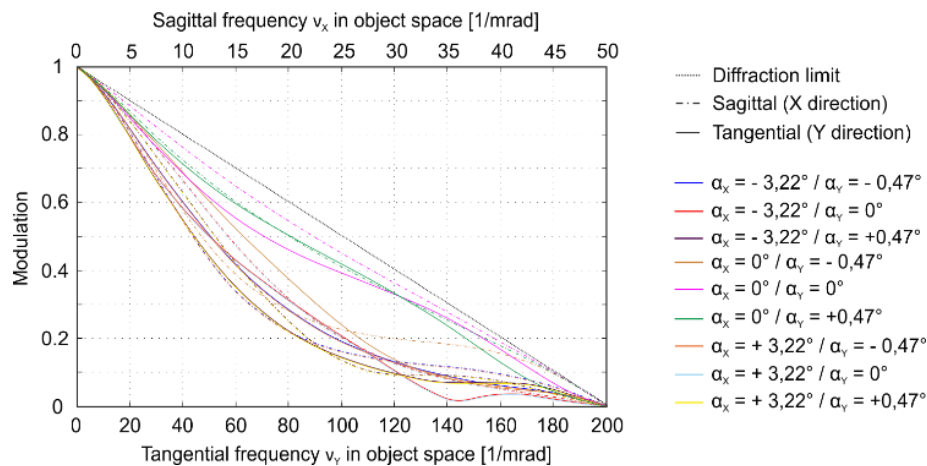

Fig. 2: Nominal telescope MTF in object space. Note the different axis for sagittal and tangential direction.

Based on the optical telescope design, optical surfaces M1 and M3, as well as M2 and M4 are mechanically coupled and processed as single platforms M1M3 and M2M4 (see Fig. 3). Both modules are developed from a single block aluminum Al6061 T6, prefabricated, lightweighted, and thermally aged. The mechanical interface to the telescope housing is formed by three ultra-precisely machined plane surfaces at the mirror substrates. Small diamond machined decoupling bipods mounted at the telescope housing are used as connecting elements between telescope structure and mirror modules. Instead of screwing both modules to the base structures, they are secured by tie rods in order to minimize mounting torques that would lead to mechanical distortions of the optical parts. The telescope housing itself is developed fully symmetrical from two shells out of Al6061. An inside ribbed structure is manufactured for both shells in a conventional milling process and is foreseen to increase mechanical stiffness and to provide stray light baffles. After heat treating the premachined material, a qualified anodizing process is used to blacken both shells before clamping them together. Three larger bipods are mounted at a spacing of about 120° and form the interface to the next higher system level. The whole telescope demonstrator reaches a size of 590 x 440 x 210 mm³ and a final mass of about 17 kg. Simulations based on finite elemente modeling show a first Eigenfrequencies of 211 Hz for an oscillation of the bipods and 237 Hz for the telescope housing.
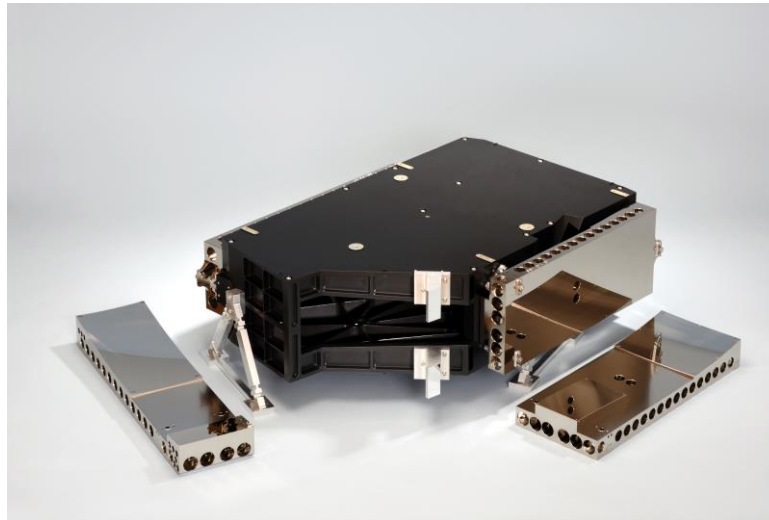
Fig. 3: Assembled telescope with two additional mirror modules M1M3 and M2M4

III. MIRROR MANUFACTURING ANALYSES

The main manufacturing steps for freeform mirror fabrication include a combined process of fast tool servo diamond turning and diamond micro milling for the generation of optical surfaces and fiducials, a Magnetorheological Finishing (MRF) step for surface error correction, and a Computer Controlled Polishing (CCP) step for surface smoothing. All of the tools address a certain spatial frequency content of the optical surfaces, both in their ability to remove or generate certain surface errors.

In the following Fig. 4, individual figure deviation as well as relative position error of both mirror modules M1M3 and M2M4 are shown after final diamond machining. Based on the simultaneous cutting of each two freeform surfaces during a single revolution of the machining spindle, an excellent relative position error between both surfaces is achieved, which already reduces the necessary degrees of freedom for the later overall telescope integration from 24 to 12. Individual figure quality ranges from about 83 nm rms for M2 up to 122 nm rms for M1 and is mainly driven by the stability of the diamond turning process over cutting time.
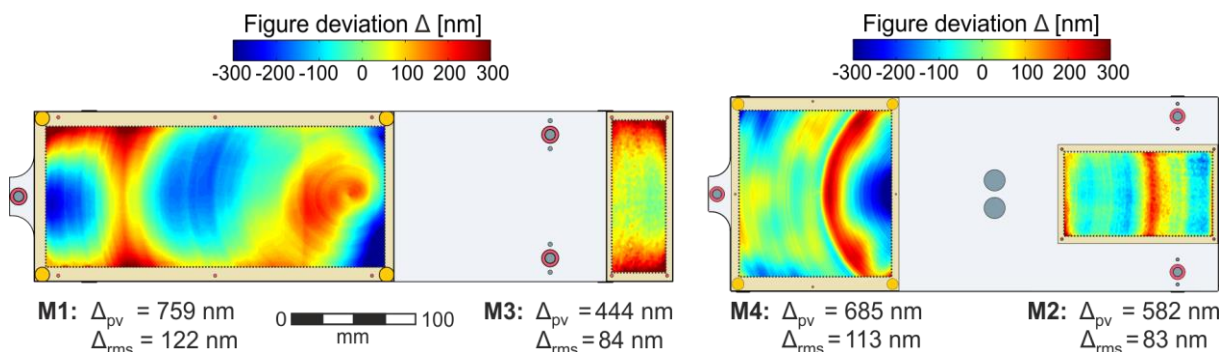

M1: Δ_{pv} = 759 nm   **M3:** Δ_{pv} = 444 nm
     Δ_{rms} = 122 nm Δ_{rms} = 84 nm

M4: Δ_{pv} = 685 nm   **M2:** Δ_{pv} = 582 nm
     Δ_{rms} = 113 nm Δ_{rms} = 83 nm

Fig. 4: Measured deviation of individual surface figure and relative position for mirror modules M1M3 (left) and M2M4 (right) after diamond turning.

Fig. 5 shows individual surface errors and individual position deviations after all freeform surfaces have been processed within several MRF figure correction loops. The individual surface errors of mirrors M1 and M4 are measured using full aperture interferometry with specialized Computer Generated Holograms [17], whereas M2 and M3 are measured by a high-resolution profilometer. Individual figure errors are remarkably reduced to values between 9,5 nm rms for M4 to 12,8 nm rms for M3. However, surface errors with spatial wavelengths between 0,5 mm to about 3 mm are nearly unaffected by the figure correction process. This is based on the size and nature of the sub-aperture MRF tool, which is on the one hand not small enough to tackle the errors by a dwell-time driven process and on the other hand too small to effectively smooth out the ripples by a polishing motion. Especially M4 shows a severe circular structure having its center at the spindle axis of the diamond turning machine [18].
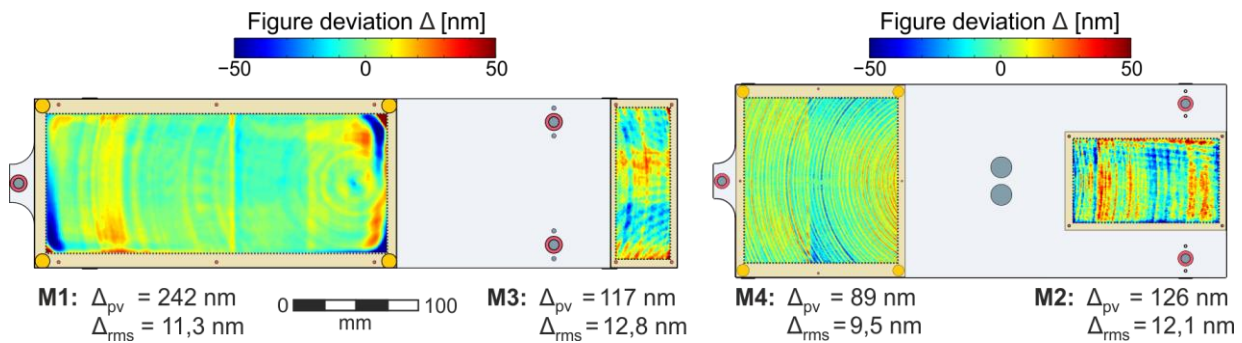
Fig. 5: Measured deviation of individual surface figure and relative position for mirror modules M1M3 (left) and M2M4 (right) after individual figure correction by MRF.

In order to further reduce this mid-spatial ripples, an additional polishing process based on a larger semi-flexible tool is applied to the four mirrors individually. Remaining surface errors are reduced to a range between 5,2 nm rms for M4 and 10,7 nm rms for M1. Fig. 6 shows that most of the diamond turning ripples have been smoothed out by the CCP step. Low-order figure errors induced by the CCP process are compensated afterwards in an additional iteration of MRF figure correction, leading to the final results shown in Fig. 6. On the other hand, also the CPP tool leaves a raster-type tool pattern in the mid-spatial regime. In order to further reduce the surface form errors, the sequence of figure correction and smoothing would have to be continued.
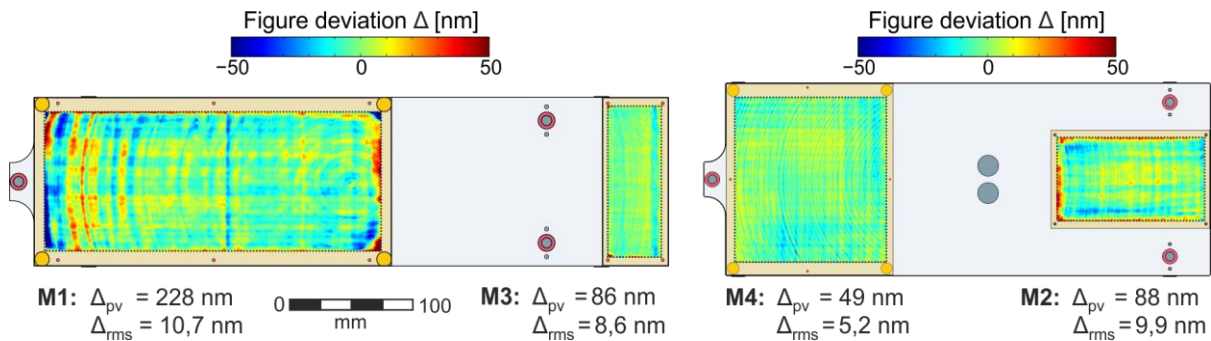

Fig. 6: Measured deviation of individual surface figure and relative position for mirror modules M1M3 (left) and M2M4 (right) CCP smoothing and figure correction by MRF.

IV. SYSTEM INTEGRATION

The modular system concept intends a simplified integration using ultra-precisely machined interfaces at all relevant components. Therefore, integration is basically reduced to attaching both modules to the telescope housing and fixing their positions at a few interfaces by applying defined mounting forces. No special alignment strategies, like an external measurement of fiducials with a coordinate measurement machine, are further necessary. The optomechanical system concept leads to a considerable reduction of the relevant 24 degrees of freedom (6 DOF for each of the freeform surfaces) that have to be considered during integration:

- The modularization precisely fixes the relative position between monolithically coupled surfaces and thus reduces the overal DOF to 12. Coupling is taken into account during tolerancing and sensitivity analysis.

- Design and geometry of the mechanical interconnections between mirror modules and telescope structure fix axial translations TZ_{M1M3}, TZ_{M2M4}, as well as rotations RX_{M1M3}, RY_{M1M3}, RX_{M2M4}, and RY_{M2M4} about the lateral mirror axes.

- Remaining 6 DOFs divide into the open translations TX_{M1M3}, TY_{M1M3}, TX_{M2M4}, and TY_{M2M4} and clocking RZ_{M1M3}, RZ_{M2M4}. Practically, one mirror module keeps fixed during integration and the position of the second one is relatively fine adjusted while measuring the optical wave aberration of the telescope.

A tolerance analysis shows that especially misalignments in axial direction TZ (air distance, fixed by mechanical interfaces) as well as translations TY (adjustable) of a few microns strongly degrade the systems wave aberration and lead to dominant low order defocus and astigmatism terms. Lateral misalignments in the two orthogonal directions lead to the same aberration types with comparable magnitudes and may cancel out if the on-axis performance is evaluated only. Therefore, measurement and analysis of the complete aberration field over the system's intended field of view is crucial to validate correct alignment and functionality.

Based on the simplified system integration approach, the telescope was integrated after each manufacturing step shown in the previous section. Results for the experimentally evaluated wave aberration are given within the next sub-chapters.

A. Telescope with diamond machined mirrors

The optical telescope performance is tested in a double-path interferometric setup under clean room conditions. A 6" Fizeau interferometer is used to illuminate the system from its exit aperture. The wave propagates through the system and is reflected at a 10" plano reference mirror. In order to evaluate the performance over the field of view, the telescope is placed via a kinematic mount on a hexapod parallel kinematic system and precisely manipulated with respect to the incoming beam.

The system is initially assembled by attaching both mirror modules at their diamond machined mounting interfaces to the diamond flycut bipods at the telescope structure. Lateral degrees of freedom are preliminary fixed using gauge blocks and mechanical stops, which are temporarily mounted to the housing. Because of the chosen modular system approach in connection with the procedure for referencing, the systems wave aberration can directly be measured and evaluated after the first assembly. During the fine alignment step, one module is kept fixed in position and the second one is iteratively adjusted by changing the dimensions of the gauge blocks. Low order aberration terms indicate remaining misalignments, which are reduced within a few adjustments in the remaining degrees of freedom. The intuitive and reproducible assembly is done within one day and verifies the implementation of the chosen snap-together mounting approach for visible applications.
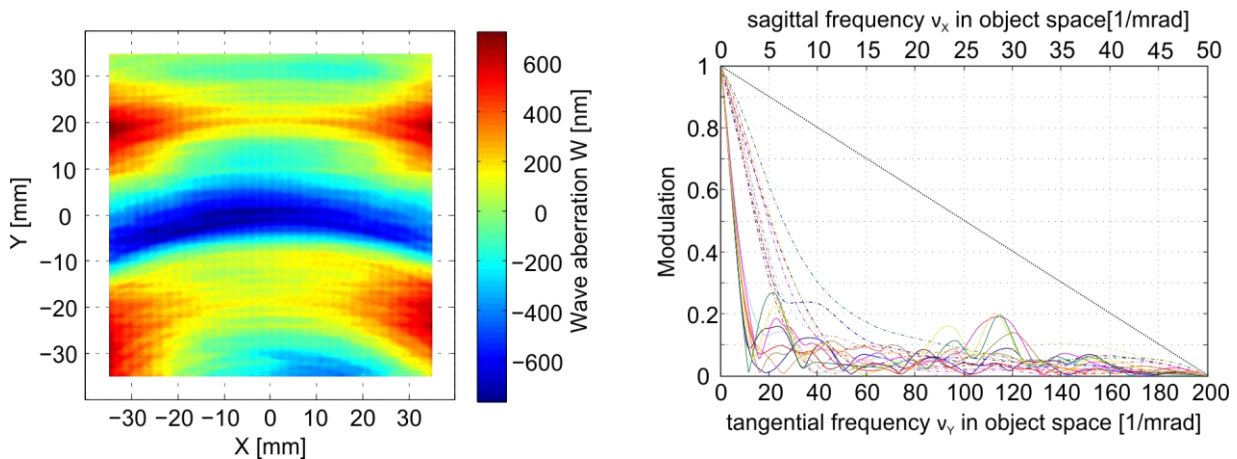

Fig. 7: Experimentally measured wave aberration of the aligned telescope with diamond machined mirror modules in the central field (left) and corresponding MTF for 9 field angles (right).

Fig. 7 shows the on-axis wave aberration of the afocal telescope as well as the measured MTF for 9 field angles. The colors in the MTF plot refer to the colors given for the theoretic MTF in Fig. 2. The on-axis wave aberration is measured to 1,51 µm p.-v. and 294 nm rms, respectively. The imaging quality is influenced mainly by the residual figure errors of the individual mirror surfaces M1 to M4, as illustrated in Fig. 4. Contributions due to residual position or alignment errors cannot be observed and are comparable small, proofing the concept of the snap-together mounting approach. Using diamond machined mirror modules only, the telescope achieves a diffraction limited performance beginning at a wavelength of about 4 µm in the IR.

B. Telescope with figure corrected mirrors

The anamorphic telescope is assembled a second time using the MRF figure corrected mirror modules according to their quality demonstrated in Fig. 5. Based on the mounting concept, the telescope could be assembled equal to the first integration within a few hours – no further adjustments were necessary. The following Fig. 8 shows again the on-axis wave aberration as well as the MTF plots at measurement wavelength of λ = 632,8 nm. Wave aberration (0,73 µm p.-v. / 83 nm rms) and MTF curves show a remarkable improvement of the telescope quality with diffraction limited performance at around 1 µm application wavelength. The imaging quality is mainly limited by two contributors, namely a field constant defocus term of about 30 nm rms and various mid-spatial frequency ripples having different magnitude and orientation.

Defocus is a result of an axial misalignment between both mirror modules M1M3 and M2M4 of about 6 µm and is in excellent agreement with optical simulations. Based on the mounting concept, axial position is defined by diamond machined interfaces and cannot be adjusted during system integration.

Imaging effects due to structured mid-spatial frequencies depend on the relative illumination and position of the ripple pattern within the optical beam path. Thus, three dominant parts of ripples can be distinguished in the wave aberration shown in Fig. 8:

- On-axis concentric rings due to remaining circular ripples on the mirror M4, which is illuminated for each field angle over a large area. Thus, ripples are imaged with almost the same lateral size to the image plane.
- A regular horizontal grid as a result of remaining polar spokes on mirror M3, which lies close to the intermediate image and is illuminated for each field angle over a narrow rectangular footprint only. The ripple structure is hence magnified and overlayed as straight horizontal lines to the image plane.
- A vertical grid due to remaining radial ripples on mirror M2, which is also illuminated over a narrow rectangular footprint orthogonal to the footprint on M3. Ripples image as a nearly straight vertical line pattern.
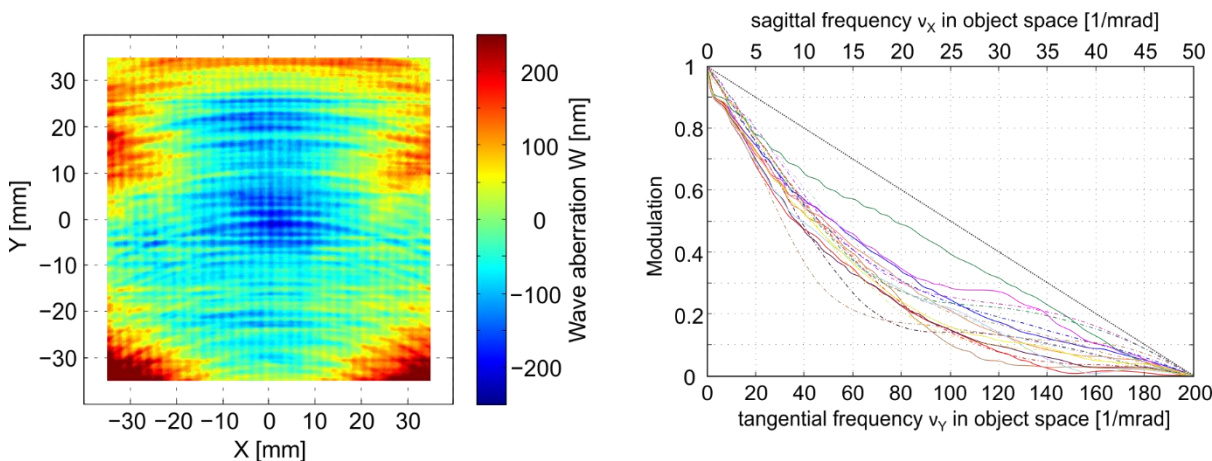

Fig. 8: Experimentally measured wave aberration of the aligned telescope with MRF figure corrected mirror modules in the central field (left) and corresponding MTF for 9 field angles (right).

C. Telescope with post polished mirrors

In order to further suppress the influence of the mid-spatial surface errors, all mirror surfaces have been post-polished and figure corrected again until they achieved the performance shown in Fig. 6. The telescope is integrated afterwards for the third time and its wave aberration is measured experimentally over the complete field of view. Fig. 9 depicts again MTF curves and the on-axis wave aberration which is measured to 882 nm p.-v. and 123 nm rms, respectively.
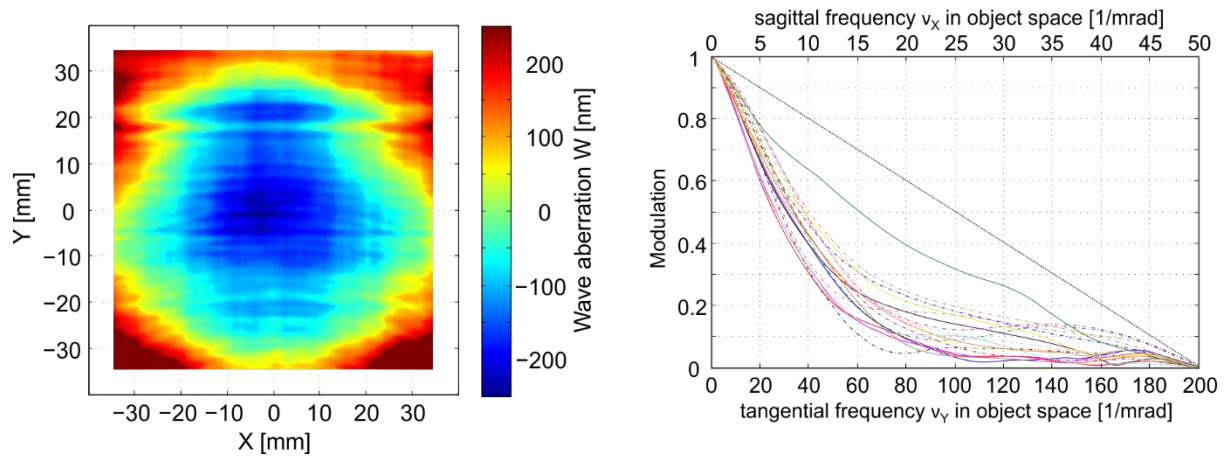
Fig. 9: Experimentally measured wave aberration of the aligned telescope with CCP polished and MRF figure corrected mirror modules in the central field (left) and corresponding MTF for 9 field angles (right).

The improvement of the individual surfaces led to a smoother wave aberration and smoother MTF curves without the characteristic ripples that have been observed using MRF figure corrected mirror modules only. The majority of the surface waviness could be smoothed out using the post polishing process. However, the field constant defocus term increased from about 30 nm rms after the second integration to about 70 nm rms after post polishing. This can be explained with the necessary amount of material removal for polishing and figure correction on all surfaces. Since the mechanical interfaces are still in its diamond machined condition, mirror vertices are shifted slightly in axial direction and the defocus term increases. Even though the individual surface performance is well below the specification required for diffraction limited imaging in the VIS, the telescope is now limited by residual position errors of the optical surfaces along the beam path.

IV. SYSTEM CORRECTION USING ONE MIRROR AS A COMPENSATOR

One opportunity to correct the residual defocus term is another diamond machining of the mounting interfaces at the telescope housing in a fly-cutting process. However, since the only remaining aberration is field constant defocus, we decided to apply another compensation approach imprinting a defined figure deviation to a selected freeform surface. The perfect position for such a system correcting surface would be either the entrance or exit pupil of the telescope. Both planes are physically not present as surfaces and thus not feasible. Mirror M4 is close to the systems pupil and is illuminated with a sufficient overlap from the different field angles of the system. After retransferring all measured wave aberrations of 121 field angles back to an optical design program, variable polynomials were added to the base shape of mirror M4 and optimized to reduce the systems wave aberration. As expected, a variation of the second-order polynomials led to a remarkable reduction of the simulated wave aberration, compensating the field constant defocus term. The simulated deviation of M4 to its design shape was used afterwards as an incoming information for another MRF figuring process and the convex deviation was imprinted to a final deviation of about 582 nm p.-v. and 145 nm rms, respectively (see Fig. 10).
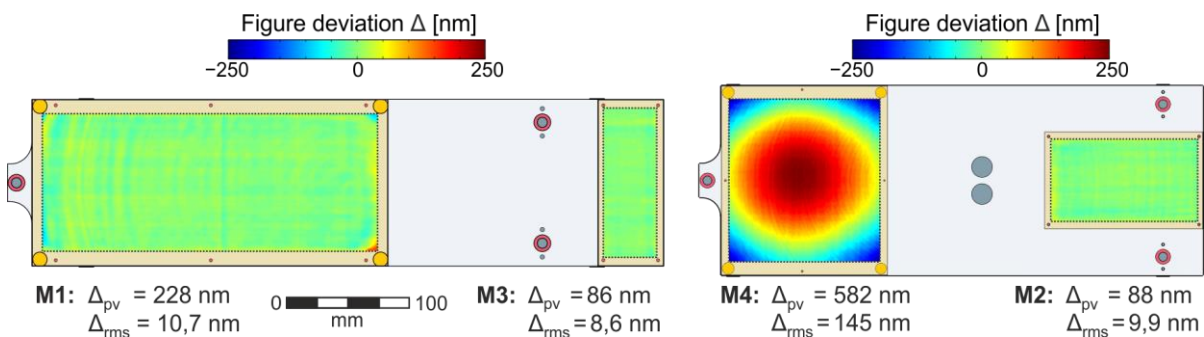.

Fig. 10: Measured deviation of individual surface figure and relative position for mirror modules M1M3 (left) and M2M4 (right) after imprinting a corrector surface on M4. All other mirrors are machined to its design surface and shown within the same color scale.
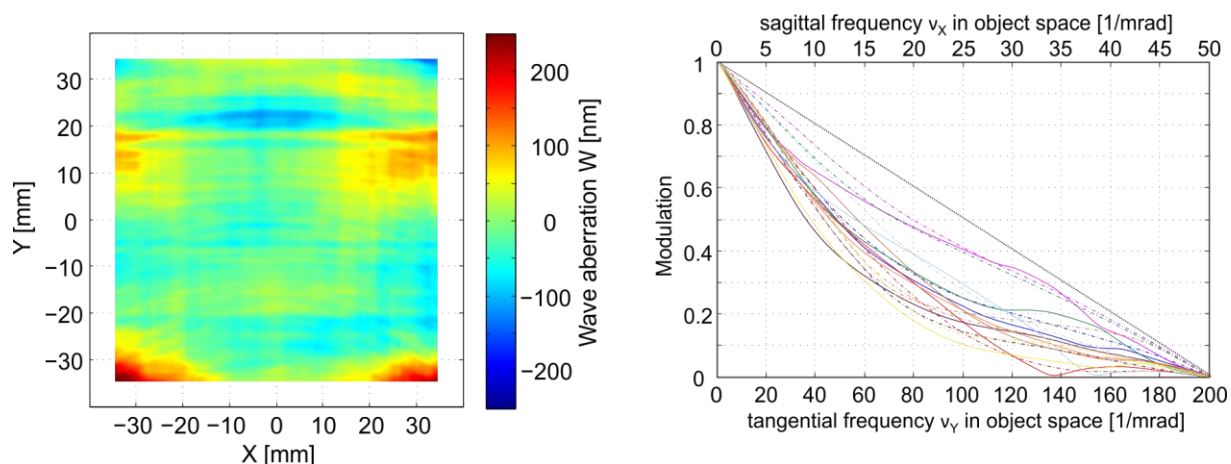
Fig. 11: Experimentally measured wave aberration of the aligned telescope in the central field (left) having a system compensating surface on mirror M4 and corresponding MTF for 9 field angles (right).

Fig. 11 shows the telescope imaging quality after mirror module M2M4 was integrated having the corrector surface on M4. Only one correction was necessary to directly measure the fully compensated on-axis wave aberration of 446 nm p.-v. and 44 nm rms, respectively. Also the MTF curves are now in very good agreement with the telescope design.

V. SUMMARY

The article presents the development, fabrication, and testing of an anamorphic imaging four freeform mirror telescope demonstrator with a 200 x 50 mm² entrance aperture and diffraction limited optical performance in the visible spectral range. Optical and mechanical design follow up approaches developed for infrared mirror optics and intend a modular fabrication of each two optical surfaces on common mechanical carriers. Manufacturing precisions achieved lead to relative position errors between two monolithically coupled surfaces well below 1 µm and enable a fast and reproducible integration of the overall telescope following a snap-together approach. Individual surface form deviations, mid-spatial waviness and high-spatial surface roughness are corrected by a combination of MRF figure correction and post polishing techniques.

Accuracy and benefits using diamond machined interfaces and fiducials for optical and tactile metrology are demonstrated. The modularization as well as the concept of referencing simplify the later integration tremendously. Design and mechanical fabrication qualities verify the achievement of excellent and stable system qualities and will play a major role during the development of future metal based mirror instrumentations for space and astronomy. It was demonstrated that the concept of a snap-together system integration is still feasible for optical telescopes having a tight tolerance budget, if additional compensating strategies are integrated.

REFERENCES

[1] Fang, F.Z., Zhang, X.D., Weckenmann, A., Zhang, G.X., Evans, C. "Manufacturing and measurement of freeform optics", CIRP Annals – Manufacturing Technology 62, 832-846 (2013).
[2] Yoder, P.R., Vukobratovich, D. "Opto-Mechanical Systems Design", CRC Press (2015).
[3] Kroes, G., Oudenhuysen, A., de Haan, M., Jager, R., Pauwels, E. „MIRI-JWST spectrometer main optics flight model realization and performance test results", Proc. SPIE 7731 (2010).
[4] Doyon, R., Hutchings, J., Beaulieu, M., Albert, L. „The JWST Fine Guidance Sensor (GGS) and Near-Infrared Imager and Slitless Spectrograph (NIRISS)", Proc. SPIE 8442 (2012).
[5] Hiesinger, H., Helbert, J. „The Mercury Radiometer and Thermal Infrared Spectrometer (MERTIS) for the BepiColombo mission", Planetary and Space Science 58, 144-165 (2010).
[6] Kaeufl, H. et al. „CRIRES: a high-resolution infrared spectrograph for ESO's VLT", Proc. SPIE 5492 (2004).
[7] Guanter, L., Kaufmann, H., Segl, K. et al. „The EnMAP spaceborn imaging spectroscopy mission for Earth observation", Remote Sensing 7, 8830-8857 (2015).
[8] Veefkind, J.P., Aben, I., McMullan, K., Förster, H., de Vries, J. „TROPOMI on the ESA Sentinel 5 Precursor: A GMES mission for global observations of the atmospheric composition for climate, air quality and ozone layer applications", Remote Sensing of Environment 120, 70-83 (2012).
[9] Steinkopf, R. et al. „Metal mirrors with excellent figure and roughness", Proc. SPIE 7102 (2008).

[10] Scheiding, S. et al. „Ultra-precisely manufactured mirror assemblies with well-defined reference structures", Proc. SPIE 7739 (2011).

[11] Risse, S., Scheiding, S., Gebhardt, A., Damm, C., Holota, W., Eberhardt, R., Tünnermann, A. „Development and fabrication of a hyperspectral mirror based IR-telescope with ultra-precisely manufacturing and mounting techniques for a snap-together system assembly", Proc. SPIE 8176 (2011).

[12] Beier, M., Hartung, J., Peschel, T., Damm, C., Gebhardt, A., Scheiding, S., Stumpf, D., Zeitner, U. „Development, fabrication, and testing of an anamorphic imaging snap-together freeform telescope", Appl. Optics 54, 3530-3542 (2015).

[13] Beier, M., Hartung, J., Kinast, J., Gebhardt, A., Burmeister, F., Zeitner, U., Risse, S., Eberhardt, R., Tünnermann, A. „Fabrication of metal mirror modules for snap-together VIS telescopes" Proc. SPIE 9633 (2015)

[14] Beier, M., Fuhlrott, W., Hartung, J., Holota, W., Gebhardt, A., Risse, S. „Large aperture freeform VIS telescope with smart alignment approach". Proc. SPIE 9912 (2016)

[15] Dumas, P., Hallock, R., Pisarski, A. "Applications and benefits of perfectly bad optical surfaces", Proc. SPIE 7102 (2008).

[16] Beier, M., Scheiding, S., Gebhardt, A., Risse, S., Eberhardt, R., Tünnermann, A. „Figure correction of freeform mirrors with well-defined reference structures by MRF", ASPE Topical Meeting on Aspheres and Freeforms (2014)

[17] Beier, M., Stumpf, D., Zeitner, U., Gebhardt, A., Hartung, J., Risse, S., Eberhardt, R., Gross, H., Tünnermann, A. „ Measuring position and figure deviation of freeform mirrors with computer generated holograms", Imaging and Applied Optics (2015).

[18] Pertermann, T., Hartung, J., Beier, M. et al. are intending to publish a paper entitled „Angular resolved power spectral density analysis for improving mirror manufacturing".